SPACE TELESCOPE SCIENCE INSTITUTE
Operated for NASA by AURA

Instrument Science Report STIS 2001-04

STIS Cycle 8 Calibration Close-out Report

Rosa I Diaz-Miller and Paul Goudfrooij on behalf of the

Spectrographs Group: Jerry Kriss (former member), Ivo Busko (Software Science Group), James Davies, Ron Downes, Linda Dressel, Brian Espey, Phil Hodge (Software Science Group), Jessica Kim, Howard Lanning (former member), Claus Leitherer (former member), Chris Long (Engineering Team), Grace Mitchell, Charles Proffitt, Kailash Sahu, David Stys, Jeff Valenti, Nolan Walborn.

STIS IDT: Bruce Woodgate, Ted Gull, Albert Boggess, Charles W. Bowers, Anthony Dnaks, Richard F. Green, Sara R. Heap, John B. Hutchings, Edward B. Jenkins, Charles L. Joseph, Mary Beth Kaiser, Randy Kimble, Steve Kraemer, Jeffrey L. Linsky, Stephen P. Maran, H. Warren Moos, Frederick Roesler, J. Gethyn Timothy, Donna E. Weistrop.

October 30, 2001

ABSTRACT

We summarize the status of the Cycle 8 calibration program for the Space Telescope Imaging Spectrograph (STIS) based on one year of on-orbit calibration observations.

1. Introduction

The Space Telescope Imaging Spectrograph continued its functions after its installation in February 1997 (***Woodgate et al. 1998***). A large number of on-orbit calibration programs for supported observing modes and to monitor the stability of SITS were completed during ***Cycle 7***. In the second Cycle (Cycle 8) a total of 28 calibration proposals were executed in a period of about 12 months to continuously monitor the spectrograph's

performance and characterize of newly supported modes. The definition and oversight of this program was led by Paul Goudfrooij, assisted by Ilana Dashevinsky and Rosa Diaz-Miller.

A grand total of 167 external and 1936 internal orbits were approved for Cycle 8 calibration program. The overall status of the orbits is shown in Table 1. Several new calibration proposals were added after the review, subject to the approval of the TTRB, to address new issues or problems. An example is 8799 which was added to calibrate the end-of-slit pseudo aperture location in order to reduce the CTE loses for point sources and compact objects. A total of 154 external and 1742 internal orbits were executed. There were 8 external and 5 internal orbits that failed. Of these, 8 external and 5 internal orbits were repeated. Also, in the course of the Cycle, 2 external and 257 internal orbits were withdrawn following proposal implementation in favor of Cycles 9 and 10 calibration programs and 3 internal contingency orbits were used for the NUV-MAMA anomalous recovery and fold distribution analysis. The NUV-MAMA safed when the Software Global Monitor event rate was exceeded on September 18, 1999. Subsequent analysis showed no degradation of the NUV-MAMA micro-channel plate (Long 1999a) (Proposal statistics courtesy of Nancy Fulton of the DDT).

Table 1. Summary of orbit allocation and use during the Cycle 8 calibration of STIS.

Cycle 8 Orbits	External Orbits	Internal Orbits
Allocated	167	1936
Executed	154	1742
Withdrawn	2	257
Failed	8	5
Repeated	8	5
Active	0	0

Some of the calibration programs in this Cycle are routine programs that have been established to monitor the stability of STIS and proactively search for problems that could impact the quality of the data obtained. Most of them continue monitoring already started in Cycle 7. These include test of initial pointing stability, reference aperture stability, target acquisition accuracy, focus stability, MSM stability, lamp flux degradation and long exposure pointing stability (***STIS TIR 98-07***).

The results of Cycle 8 calibration proposals are summarized in Table 2. Details for each proposal are given in the page number listed in the last column. For ease of manage-

ment of the calibration program the proposals were divided into logical groups, such as CCD Monitoring. Each group of proposals had a Calibration Analysis Team (CAT) which was assigned responsibility for the data analysis and products. Presentation of the proposals are therefore grouped by CAT group. For the Time Used (columns 3 and 4), we have summarized both the executed orbits, and the allocated orbits in square brackets [], on a proposal by proposal basis. To keep the size of the Phase 2 proposals manageable (for implementation purposes), particularly for the routine monitoring proposals (e.g. the CCD Dark Monitor), it was often necessary to split one particular aspect of the calibration into several separate Phase 2 proposals. While these were tracked separately, and are presented as separate proposals in the table, they are in fact parts of the same calibration and are not treated as separate entities in the detailed forms following the table. The forms summarize the following five items:

1. Execution: success and frequency of proposal observations.
2. Summary of Goals: Purpose of calibration
3. Summary of Analysis: highlights of the results and products, includes references for detailed analysis, procedures and/or requirements.
4. Accuracy Achieved: accuracy of the result or data processed using the calibration product.
5. Continuation Plans: follow-up calibration proposals or analysis.

Changing priorities and demands of the astronomy community influenced the course of the analysis and resulting products, which include some Cycle 9 calibration overlap. The primary products of the Cycle 8 calibration program were calibration reference files delivered to the OPUS Pipeline, SITS Instrument Science Reports (ISRs), STIS Technical Instrument reports (TIRs) and updates to the STIS Instrument Handbook (IHB). Other products include the STIS Quick-Look Analysis Reports, which are only available from the STIS Internal Calibration Programs web site (***http://www.stsci.edu/instruments/stis/calibration/***), and the STIS IDT Post-Launch Quick-Look Analysis Reports available from the STIS IDT web site (***http://hires.gsfc.nasa.gov/stis/stispage.html***). The reference file products for individual proposals are identified by their suffix, listed in the Reference File History site (***http://www.stsci.edu/instruments/stis/calibration/reference_files/oref.html***). The STIS ISRs, TIRs, and IDT analysis reports are referenced by number (e.g. ISR2001-01). The author and date may be found in Appendix A. The STIS Quick-Look Analysis Reports and TIRs are only available from the STIS internal web site, which has restricted access.

The highlights of the results of the Cycle 8 calibration program include:

1. The CTE loss for point sources is found to increase significantly with time and decreases strongly with increasing source intensity and with increasing sky background,

2. Successful commanding and calibration of the new pseudo-apertures that reduce CTE losses for observations of compact targets,
3. New wavelength setting of 2125 A for the prism was added,
4. Updated spectroscopic sensitivity reference files,
5. Repeller-wire-off mode, which suppresses the wings in the FUV line spread function was made available,
6. Updated reference files for incidence-angle corrections for non-concentric NUV-MAMA apertures,
7. Measurements of the LSF for the MAMA Echelle modes and creation of a CCD PSF library,
8. Construction of on-orbit D-flats for selected NUV-MAMA and FUV-MAMA modes,
9. Improved MAMA and CCD dispersion solutions,
10. The routine production of weekly dark and bias reference files for the CCD.

Monitoring programs are continued in cycles 9 and 10. There are, however, Cycle 8 results that led to modifications in future calibration programs or the implementation of new monitoring programs or proposals. An example of the latter is Cycle 9 proposal 8891, which verifies the centering of the end-of-slit pseudo-apertures calibrated in program 8799. Degradation of the charge transfer efficiency (CTE), on the other hand, required the implementation of new Cycle 9 monitoring programs like 8851 and 8854, that monitor the loss in CTE for point-like sources (for both, gain =1 and gain = 4) and 8839 that determines the CTE effect on extended sources. Low S/N and possible variability of the faint standard stars observed in program 8810 led to program 8849 in Cycle 9.

At the completion of this report, 4 calibration proposals are still outstanding. In some cases the analysis has been delayed pending data to be taken in future Cycles (e.g. proposal 8423 "CCD Faint Standard Extension") and/or deferred to future cycles (proposals 8428 and 8429 "MAMA FUV and NUV Flats"). In the latter case the visits in a second epoch of observations were withdrawn because the decline in the Deuterium and Krypton lamp outputs and a desire to preserve their lifetime. Proposal 8423 is continued with proposal 8849 to check for variability and to improve S/N. There is one case, proposal 8434 "MAMA Slitless Spectroscopy", for which the analysis is still pending.

2. CCD Monitoring and Detector Calibration

Table 2. STIS Cycle 8 Calibration Closure Summary

ID	Proposal Title	Time Used (orbits) executed [allocated]		Products	Accuracy Achieved	Page
		"External"	"Internal"			
CCD Monitoring and Detector Calibration						
8407	CCD Performance Monitor		42 [42]	CCD reference files; BIA and DRK ***reference files***	gain measured to 1% (unbinned), 1%-3% (binned); read noise measured to 1%-3% (unbinned), 2%-4% (binned)	page 8
8408 8437	CCD Dark Monitor		729 [854]	DRK *reference files*; ***TIR2000-06***	S/N ~ 15 dark current ~0.0035 electrons/s/pixel	page 9
8409 8439	CCD Bias Monitor		361 [428]	BIA *reference files*; ***ISR 99-08***; ***TIR2000-05***	S/N > 1.0 per pixel	page 10
8410	CCD Hot Pixel Annealing		65 [75]	*monthly reports*	monthly anneals annealed out 80 ± 35 % of hot pixels (> 0.1 e-)	page 12
8411 8797	CCD Spectroscopic Flats		72 [74]	*reference files*	temporary variations < 1%; average rms variations 0.7%	page 13
8412	CCD Imaging Flats		17 [19]		temporal variation < 1%; pixel-to-pixel fluctuation 0.4%	page13
8413	CCD Dispersion Solutions		7 [7]	DSP *reference files*	see report	page 14
8414	CCD Sparse-field CTE Internal		105 [105]	Kimble et al. (2000)	1% for signal levels > 200 electrons at center of detector	page 16
8415	CCD Sparse-field CTE external	7 [6]		CTE Workshop Proc.; ***IHB***; ISR (Goudfrooij).	1% for signal levels > 200 electrons at center of detector	page 18
8416	CCD Full-field Sensitivity	2 [4]	2 [0]	ISR in progress (Mobasher)	Changes in mag. < 1%. Repeatability of bright stars ~1%; faint stars ~ 3%	page 19
8417	Slit Wheel Repeatability		1 [1]	STIS Quick-Look report 8417	0.01 pixels or 0.5 milli-arcsec	page 20
8418	CCD Sensitivity Monitor	10 [10]		***ISR 2001-01***	$\sigma \sim 2 \times 10^{-3}$	page 22
8798	CCD Read Noise Monitor		4 [4]		+/- 0.05 DN	page 22
CCD Special Calibration Programs						
8419	CCD Coronographic PSF	15 [15]		ISR in preparation (Proffitt/IDT)		page 23

Table 2. STIS Cycle 8 Calibration Closure Summary

ID	Proposal Title	Time Used (orbits) executed [allocated]		Products	Accuracy Achieved	Page
		"External"	"Internal"			
8810	Prism Sensitivity and Faint calibration Standard Extension	2 [2]		1DT, DSP, IAC, LMP, PCT, PHT *reference files*	sensitivity ~2% relative to first order modes; wavelength 0.2 pixels in central rows.	page 24
8799	Calibration of STIS End of Slit Pseudo-Aperture Locations	3 [3]		STIS Cycle 10 Phase II Update	Slit centers within 0.1 pixels. Slit angles within 0.05-0.1 degrees.	page 24
CCD & MAMA Monitoring and Detector Calibration						
8421	Spectroscopic Sensitivity	40 [40]		PHT *reference file*s	Low and Medium resolution: 1% per resolution element (except for extreme wavelengths) High resolution: global accuracy of 2%	page 25
8422	Imaging Sensitivity & PSF Library	14 [14]		ISRs in process (Proffitt)	Imaging modes 5% in absolute flux calibration	page 26
8423	FASTEX Faint Standards Extension	16 [16]		Analysis ongoing	First order 1% Prism 10%	page 27
8424	MAMA Sensitivity & Focus Monitor	26 [26]		***STIS ISR2001-01***	MAMA modes: sigma of mean ~$4x10^{-3.}$ Average sigma of trend 0.40.	page 27
8425	MAMA Full-Field Sensitivity	6 [6]		ISR in preparation (Mobasher/Proffitt)	RMS scatter: Bright stars NUV-SRF2 1%; FUV-25MAMA 3%. Faint stars FUV-25MAMA 5%. FUV images -3%/year. FUV-F25QTZ -2%/year.	page 28
8426	MAMA Dark Monitor		226 [260]	ISR in process (Proffitt)	NUV-MAMA: 1e3-1.7e3 counts/sec FUV-MAMA: lower right corner 4 counts/low-res-pix/sec; glow region 24 counts/low-res-pix/sec	Page 29
8427	MAMA Fold distribution		4 [4]	Engineering White Paper 01-024	No degradation: measurements within 20% of past results.	page 31
8428	MAMA FUV flats		10 [18]	Analysis in progress.	expected 1% per low resolution element	page 32
8429	MAMA NUV flats		11 [20]	Analysis in progress.	expected 1% per low resolution element	page 33
8430	MAMA Dispersion Solutions		20 [20]	DSP *reference file*		
MAMA Special Programs						
8431	MAMA Repeller Wire	3 [5]	2 [5]	IDT report	Increase LSF encircled fraction in dispersion direction from 0.72 to 0.82 at 1234A and from 0.79 to 0.84 for wavelength > 1416A. Reduction total sensitivity by 35%	page 34

Table 2. STIS Cycle 8 Calibration Closure Summary

ID	Proposal Title	Time Used (orbits) executed [allocated]		Products	Accuracy Achieved	Page
		"External"	"Internal"			
8433	MAMA Incidence Angle Corrections	0 [9]	9 [0]	IAC *reference file*	0.5 - 1p ~pixel for 6X0.2 aperture <0.2 for 0.1X0.2, 0.1X0.03, 0.1X0.09 apertures	page 35
8434	MAMA Slitless Spectroscopy	9 [9]		Analysis in progress		page 34
8435	MAMA Echelle LSF Measurements	4 [4]		ISR in preparation (Sahu)	accuracy is limited by the available PSFs	page 36
TOTAL ORBITS EXECUTED Number of Allocated Orbits		**154 [167]**	**1742 [1936]**			

Proposal ID 8407: CCD Performance Monitor

Execution	Dark frames in 2x2 binning mode were taken once in July 1999. All other observations were made twice during the cycle, in February and June 2000. (The intended 6 month interval was changed by the safing of the telescope)
Summary of Goals	Measure bias level, read noise, and gain at many combinations of gain and binning to update the ccd reference files. Make bias and dark reference files at the lesser used combinations of gain and binning not covered by the daily dark and bias programs. Measure CTE using the EPER method.
Summary of Analysis	The analysis is the same as for the previous cycle, described in ***ISR 98-31*** and Kimble et al. 1998. The products include ccd, bia, and drk reference files. The measurements for the ccd reference files are given in table 1.
Accuracy Archived	Gain was measured to 1% for the unbinned pixel format, and from 1% to 3% for the binned pixel formats. Read noise was measured to 1% to 3% for the unbinned pixel format, and from 2% to 4% for the binned pixel formats. Bias level was measured to 1 ADU.
Continuation Plans	Continued without change in programs 8836.

Table 3. CCD bias level, gain, and readnoise in Feb and June 2000

Month	Gain	Binning	Bias level (ADU)	Gain (electrons/ ADU)	Read Noise (electrons)
Feb	1	1x1	1339	0.995 +/- 0.008	4.42 +/- 0.06
Jun	1	1x1	1345	0.995 +/- 0.008	4.23 +/- 0.05
Feb	1	1x2	1338	0.994+-0.008	4.32+-0.09
Jun	1	1x2	1341	0.983+-0.011	4.10+-0.10
Feb	1	2x1	1123	0.984+-0.011	3.93+-0.07
Jun	1	2x1	1130	1.003+-0.016	3.74+-0.09
Feb	1	2x2	1124	1.015+-0.025	4.22+-0.17
Jun	1	2x2	1127	1.014+-0.032	3.87+-0.14
Feb	1	4x1	1022	1.001+-0.021	4.21+-0.12
Jun	1	4x1	1022	1.066+-0.031	3.99+-0.18
Feb	1	4x2	1020	1.010+-0.017	4.19+-0.16
Jun	1	4x2	1023	0.983+-0.027	3.83+-0.14
Feb	2	1x1	1562	2.003+-0.022	5.58+-0.15
Jun	2	1x1	1565	2.000+-0.016	5.73+-0.18
Feb	4	1x1	1511	4.014+-0.032	7.43+-0.23
Jun	4	1x1	1512	4.017+-0.031	7.44+-0.20
Feb	8	1x1	1554	8.148+-0.084	13.01+-0.38
Jun	8	1x1	1554	8.146+-0.088	12.21+-0.31

Proposal ID 8408, 8437: CCD Dark Monitor

Execution	Executed twice per day (8408 in the first half of the cycle, 8437 in the second half) except during the period when the telescope was safed.
Summary of Goals	Produce weekly dark reference files from a series of long dark exposures (1100 s). Take several short dark exposures daily which observers can use to update the hot pixel intensities in the weekly dark reference files using the stsdas script ***daydark***.
Summary of Analysis	Data taken between monthly anneals is combined to produce a baseline dark image. Weekly reference dark files are made by using weekly data to update the hot pixels in the baseline dark image. The bias reference image for the corresponding time range is used to remove the bias from the dark reference frame.
Accuracy Archived	Median dark current gradually increased from 0.003 to 0.004 electron/s/pix during the cycle. This is the iterated median after up to 30 rejections of points beyond +/- 5 sigma. Signal to noise for the median count rate, for a combination of about 56 exposures of 1100 s each in the baseline dark, thus ranged from 14 to 16.
Continuation Plans	Continued without change in the cycle 9 e CCD Dark Monitor programs 8837 and 8864.

Figure 1: Dark reference file for one week in August, 1999. The display saturates at 1.0 ADU/pixel/s, which is 10 times the level at which pixels are tagged as hot (DQ=16).

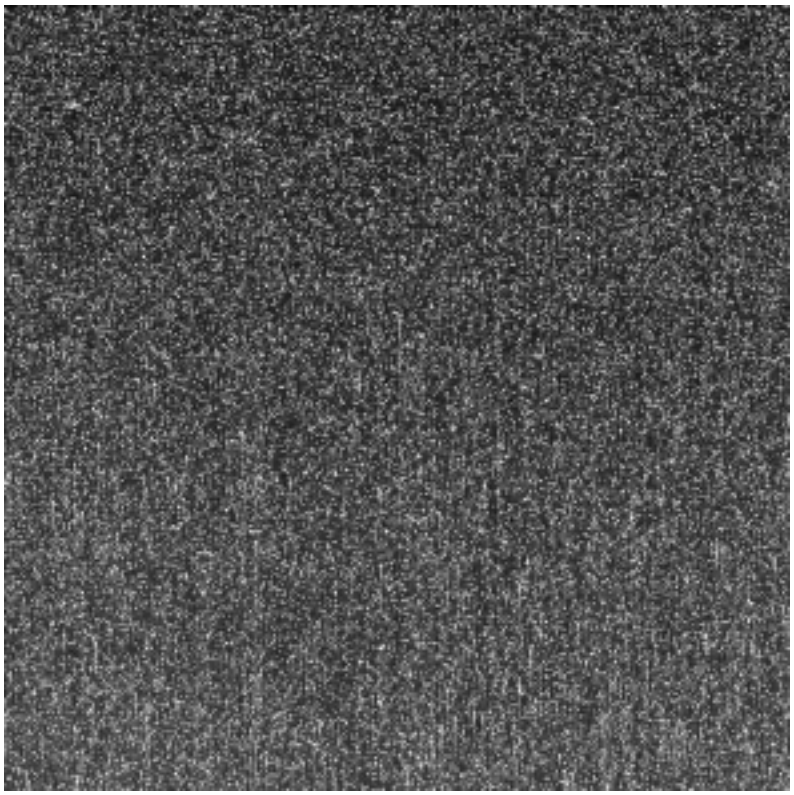

Proposal ID 8409, 8439: CCD Bias Monitor

Execution	Executed once per day (8409 in the first half of the cycle, 8439 in the second half) except for 1 week in July 1999 and during the period when the telescope was safed.
Summary of Goals	Produce bias reference files for gain 1 unbinned (weekly files) and gain 1 binned 1x2, 2x1, 2x2 (biweekly files) and gain 4 unbinned (biweekly files). Achieve signal to noise good enough to measure hot columns on these time scales.
Summary of Analysis	Bias file production is described in ***ISR 99-08*** and ***TIR 2000-05***. Data taken between monthly anneals is combined weekly (gain 1 unbinned) or biweekly to produce bias reference files. If a weekly or biweekly time period is short of data, the data from that time period are used to update hot columns in a baseline bias image, made from all data taken during that anneal period. This combination thus provides good signal-to-noise in normal columns while updating hot columns.
Accuracy Archived	This program was designed to achieve a signal-to-noise of approximately 1 per pixel for each bias reference file.
Continuation Plans	Continued without change in the Cycle 9 CCD Bias Monitor programs 8838 and 8865.

Figure 2: Bias reference file for one week in August, 1999. The display saturates at 6.5 ADU/pixel.

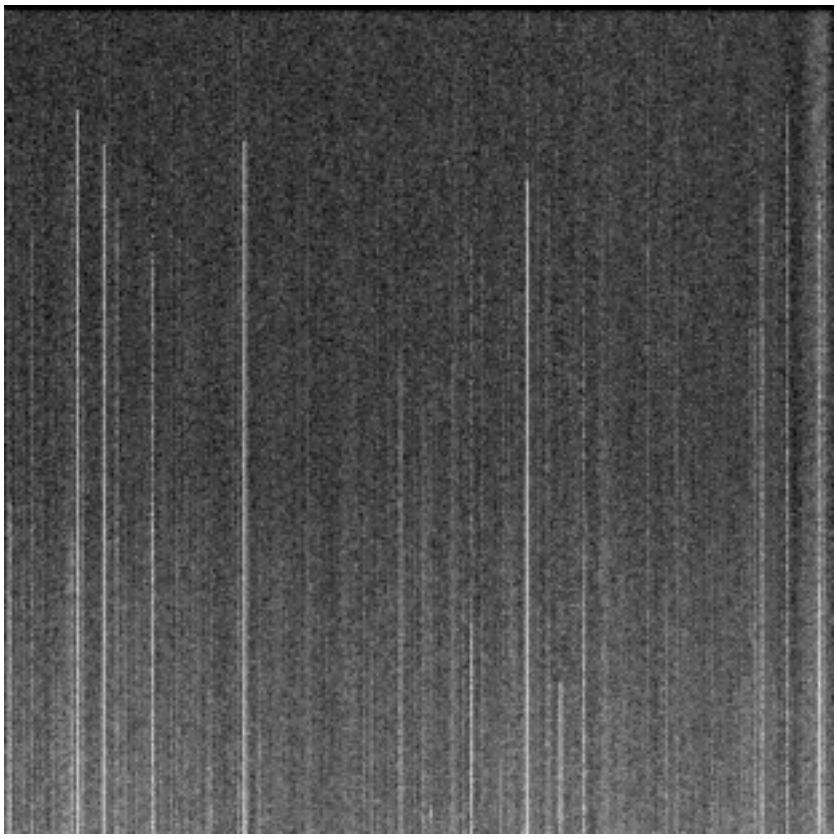

Table 4. Median bias level, read noise, and signal-to-noise for bias reference files at the beginning of cycle 8 (first entry) and following SM3B (second entry).

gain	binning	median (ADU)	read noise per exposure (ADU)	number of exposures combined	read noise in ref file	S/N per pixel in ref file
1	1x1	0.56	4.0	98	0.40	1.4
		0.64	4.5	98	0.45	1.4
1	1x2	0.85	4.1	28	0.77	1.1
		0.95	4.4	28	0.84	1.1
1	2x1	0.71	3.8	28	0.72	1.0
		0.88	4.0	28	0.76	1.2
1	2x2	1.37	3.7	28	0.70	2.0
		1.41	4.1	28	0.78	1.8
4	1x1	1.52	1.7	42	0.26	5.8
		1.53	1.8	42	0.28	5.5

Proposal ID 8410: CCD Hot Pixel Annealing

Execution	Groups of three visits executed approximately once every four weeks between July 1999 and August 2000. November and December 1999 visits were not executed because of the HST safing and were not repeated. All other visits executed successfully.
Summary of Goals	Anneal the STIS CCD and monitor the effectiveness of the anneal by taking pre- and post-anneal dark images
Summary of Analysis	Reports and figures summarizing the anneal results are posted monthly on the internal-only page ***http://www.stsci.edu/instruments/stis/calibration/Monitors/anneal***. Between anneals hot pixels at the 0.1 e/s level increased by about 41 per day. Post-anneal hot pixels increased at an average rate of 9.1 per day at the 0.1 e/s level during cycle 8; this is slightly smaller than the rate of about 12 per day during cycle 7. As of August 2000, there were 15471 post-anneal hot pixels with > 0.1 e/s, 3146 > 1.0 e/s, and 354 > 10 e/s. The extended HST safing in late 1999 does not appear to have had any significant effect on the CCD anneal results.
Accuracy Archived	The monthly anneals in this proposal annealed out 84+/-35 percent of the new hot pixels (>0.1 e-) created each month.
Continuation Plans	Continued by 8841, STIS CCD Hot Pixel Annealing C9.

Figure 3: The number of hot pixels found shortly after each monthly anneal of the CCD is shown as a function of time. This figure includes some data from the cycle 9 follow on program 8841.

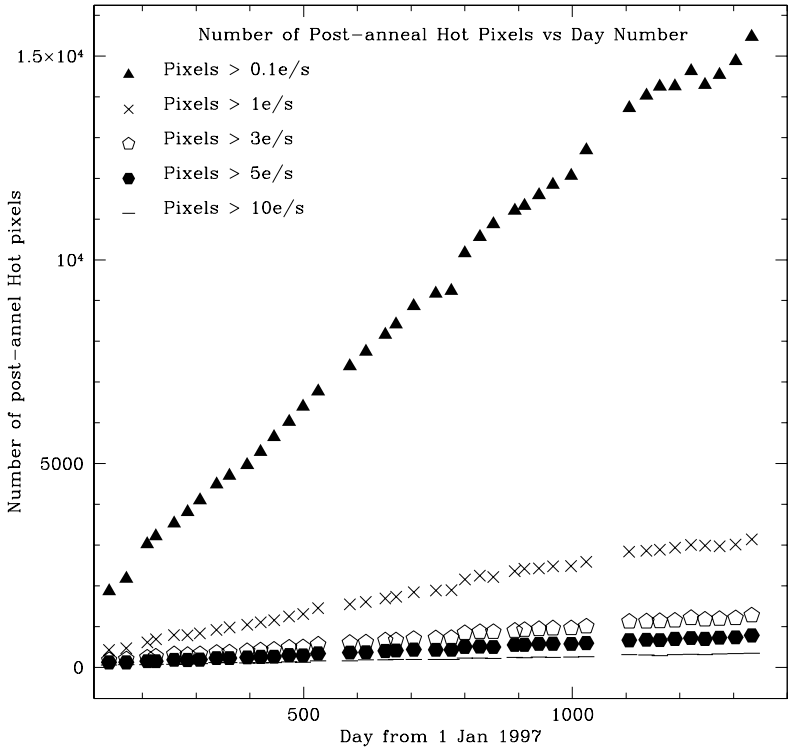

Proposal ID 8411, 8797: CCD Spectroscopic Flats

Execution	Visits successfully completed in August 2000
Summary of Goals	The purpose of this program is to take a series of internal flats in spectroscopic mode for delivery to the STIS pipeline. The program is aimed to achieve good S/N at all wavelengths by taking a number of exposures with different gratings. The tungsten and deuterium lamps are used.
Summary of Analysis	For observations taken with a slit, the fiducial bar is placed at 5 different positions in the image so that they can be removed in a combined flat. At least 5 iterations are made for each exposure for cosmic ray removal. One grating is monitored monthly for changes (G430M, 5216 Angstroms, GAIN=1 and 4), using the Tungsten lamp. The others are measured once in the cycle at GAIN=4.
Accuracy Archived	a) the temporal variation in the CCD flats is consistent with < 1% per year. b) the intrinsic rms fluctuation in the CCD flat-field is, on average, 0.7%. This indicates the level to which one could improve the noise behavior in the spectra by flatfielding.
Continuation Plans	Cycle 9 continuation program 8845

Proposal ID 8412: CCD Imaging Flats

Execution	Visits successfully completed in August 2000
Summary of Goals	The purpose of this program is to take a series of CCD flats using the mirror and aperture every month to monitor the characteristics of the CCD response. Also look for the development of new cosmetic defects. Flats for F28X50OII and F28X50OIII were also taken.
Summary of Analysis	The internal flatfields were obtained for 50CCD and F28x50LP in a monthly basis, using Tungsten lamps. The F28XOII and F28XOIII flats were taken once every 6 months. The flats were analyzed the same way as the data over the previous years.
Accuracy Archived	A temporal variation of < 1% is found in the imaging flats. A pixel-to-pixel fluctuation of 0.4% is found.
Continuation Plans	Cycle 9 continuation program 8846.

Proposal ID 8413: CCD Dispersion Solutions

Execution

Program executed twice: 2 -- 3 Aug 1999, 1 -- 2 Aug 2000

Summary of Goals

Obtain deep engineering wavecals for all CCD gratings (G750L, G750M, G430L, G430M, G230LB, G230MB) at the prime wavelengths using the 52x0.1 slit. Implement improved solutions if necessary.

Summary of Analysis

Revised dispersion solutions for MAMA and CCD first order modes were received from Don Lindler during Cycle 8 and listed in Table 5. These solutions are based upon measurements of many observations, including those from this program. The new dispersion solutions improve on the existing ones in two ways: a) they now incorporate a cubic term in the equation that allows for a better fit to the dispersion curve, and: b) they better represent the dispersion solutions across the whole of the detector, i.e. at points other than near the center line. Engineering wavecals from the database used by Lindler were extracted from the archive and 1-D spectra extracted at both Y = 512 and Y = 900 for each setting. These spectra were self-calibrated using the method outlined in ***ISR 1998-12*** and measured line locations compared with the wavelengths listed on the spectral trace plots. In Table 5 the number of lines used to determine the solutions is given in the column “n”.

Note that both the G230MB 2416 and G230MB 2697 settings are vignetted at the Y = 900 location and therefore no lines could be measured. Some other settings also suffered from vignetting, but some lines were measurable.

Accuracy Archived

The accuracy of dispersion solutions along Y = 512 pixels is slightly improved relative to the existing solutions and the rms values range from 0.3 pixels for the G230LB/G230MB settings to 0.1 pixels for the G750L/G750M settings. Values for positions close to Y = 900 pixels are much improved over the existing solutions, and generally have an rms of less than 0.3 pixels. Exceptions are the G230MB 1713 and G230LB 2375 modes that have rms values of 4.1 and 1.4 pixels, respectively.

The G230MB 1713 setting shows a trend in residuals of both current and new calibration with wavelength, with the offset (observed-true) decreasing from roughly 0.7 Angstroms at the short wavelength end to 0.0 Angstroms near the long wavelength end.

For the G750M 10363 (unsupported) setting, the measurements show a clear trend in residuals (in the sense of observed - true) from approximately -1.5 Angstroms at the blue end to approximately 3.5 Angstroms at the red end.

For both these settings, the trend in residuals leads to an inflated rms for the dispersion measurements.

NOTE: The mean wavelengths for data extracted from Y = 512 for the following settings are offset from the laboratory value by more than 3 pixels:

Mode	wavecen	rootname
G430M	3680	o5iz02coq
G430M	4961	o5iz02cqq
G430M	5471	o5iz02crq
G750M	10363	o5iz01deq

This appears to be due to an offset in the reference lamptab file. Spot checks show that the wavelengths given in the spectral trace plots (from which the laboratory wavelengths used for this calibration testing were taken) are correct.

Continuation Plans

Cycle 9 proposal 8848

Table 5. Table of measured offsets measured at Y = 512 and Y = 900 for both current and new dispersion solutions.

				current 512			new 512			current 900			new 900		
rootname	**Mode**	**cenwave**	**A/pix**	**mean**	**sigma**	**n**	**mean**	**sigma**	**n**	**mean**	**sigma**	**n**	**mean**	**sigma**	**n**
o5iz04d2q	G230LB	2375	1.35	0.405	0.303	7	0.276	0.157	7	2.084	0.252	3	-0.798	0.153	3
o5iz03hsq	G230MB	1713	0.15	0.017	0.029	5	0.007	0.021	5	0.717	0.292	5	0.225	0.347	5
o5iz04d3q	G230MB	1995	0.15	0.019	0.031	9	0.003	0.016	9	0.369	0.061	4	0.061	0.033	4
o5iz04d4q	G230MB	2416	0.15	0.001	0.034	5	-0.001	0.035	5	.....	...	...	.....	...	...
o5iz04d5q	G230MB	2697	0.15	0.047	0.059	4	0.022	0.049	4	.....	...	...	.....	...	...
o5iz04d6q	G230MB	3115	0.15	0.014	0.018	5	0.005	0.015	5	0.263	0.065	5	0.024	0.041	5
o5iz02cmq	G430L	4300	2.73	1.150	0.795	6	0.395	0.598	6	3.093	0.956	6	2.460	1.078	6
o5iz02cnq	G430M	3165	0.28	0.924	0.067	8	0.897	0.051	8	1.165	0.070	8	0.962	0.058	8
o5iz02coq	G430M	3680	0.28	1.026	0.051	6	1.051	0.075	6	1.303	0.082	6	1.129	0.069	6
o5iz02cpq	G430M	4194	0.28	-0.094	0.026	6	-0.089	0.019	6	0.125	0.040	6	0.015	0.036	6
o5iz02cqq	G430M	4961	0.28	1.371	0.073	6	1.370	0.041	6	1.681	0.088	6	1.409	0.032	6
o5iz02crq	G430M	5471	0.28	1.506	0.054	7	1.502	0.028	7	1.648	0.12	7	1.556	0.47	7
o5iz01d8q	G750L	7751	4.92	2.109	0.353	10	1.378	0.516	10	4.648	0.489	10	3.453	0.905	10
o5iz01d9q	G750L	8975	4.92	2.904	0.471	8	1.905	0.366	8	5.418	1.123	7	3.975	1.185	7
o5iz01daq	G750M	5734	0.56	-0.024	0.017	3	-0.017	0.032	3	0.881	0.042	3	0.154	0.068	3
o5iz01dgq	G750M	6581	0.56	0.036	0.014	5	0.032	0.017	5	0.452	0.104	5	0.174	0.018	5
o5iz01dbq	G750M	6768	0.56	-0.005	0.077	7	0.004	0.046	7	0.401	0.091	7	0.074	0.018	7
o5iz01dcq	G750M	8311	0.56	2.306	0.077	7	2.269	0.040	7	2.670	0.069	7	2.416	0.098	7
o5iz01dhq	G750M	8561	0.56	-0.004	0.054	7	0.00	0.042	7	0.320	0.119	7	0.149	0.063	7
o5iz01ddq	G750M	9336	0.56	0.001	0.039	8	-0.036	0.049	8	0.354	0.026	8	0.109	0.027	8
o5iz01deq	G750M	10363	0.56	-0.637	1.316	10	-0.709	1.253	10	3.369	0.0	1	2.909	0.0	1

Proposal ID 8414: CCD Sparse-Field CTE Internal

Execution	Visits 1-40 executed successfully during Sep 6 - 7, 1999; Visits 41-5W executed successfully during Apr 11 - 17, 2000; Visits 71-7W executed successfully during Aug 21 - 30, 2000
Summary of Goals	Measure Charge Transfer Efficiency (CTE) for point-like sources in a sparse field along the parallel register, as a function of source intensity. Use bi-directional clocking method.
Summary of Analysis	A sequence of nominally identical exposures is taken, alternating the read-out between amplifiers on opposite sides of the CCD. After correcting for gain differences in the read-out chains, the observed ratio of the fluxes seen by the two amplifiers can be fit to a simple model of constant fractional charge loss per pixel transfer. By fitting the observed flux ratio at a range of source positions along the columns, one can confirm that what is being measured is indeed a charge transfer effect. This "internal" version of the "sparse field test" is as follows. Using an onboard tungsten lamp, the images of a narrow slit is projected at five positions along the CCD columns. The data from this program are representative of "worst-case" spectroscopic observations, since there is essentially no sky background to provide any filling of charge traps in the image array. At each position, the alternating sequence of exposures mentioned above is taken. For each exposure, the average flux per column within a standard 7-row extraction aperture and the centroid of the image profile within those 7 rows is calculated. The alternating exposure sequence allows CTE effects to be separated from warmup effects of the calibration lamp. Derived CTI (Charge Transfer Inefficiency) values (and corresponding charge loss when transferring from row 512 of the CCD) are plotted for the 8414 and earlier data. In-flight degradation from the pre-flight CTI values is apparent. As a function of signal level, the fractional charge loss (proportional to CTI) decreases with increasing signal level. More detailed analysis is described in Kimble, Goudfrooij & Gilliland (2000, SPIE, 4013, 532).
Accuracy Archived	CTE loss accurate to within 1% for signal levels > 200 electrons at the center of the CCD.
Continuation Plans	Continued as Cycle 9 proposal 8851.

Figure 4: (a) Parallel CTI and corresponding percentage charge loss when clocking from field center, derived from the internal sparse field test, from pre-flight measurements and from three epochs in flight. (b) The parallel centroid lag suffered by a 2-pixel FWHM input image when clocking from field center. These results are applicable to spectroscopy of point sources with low background.

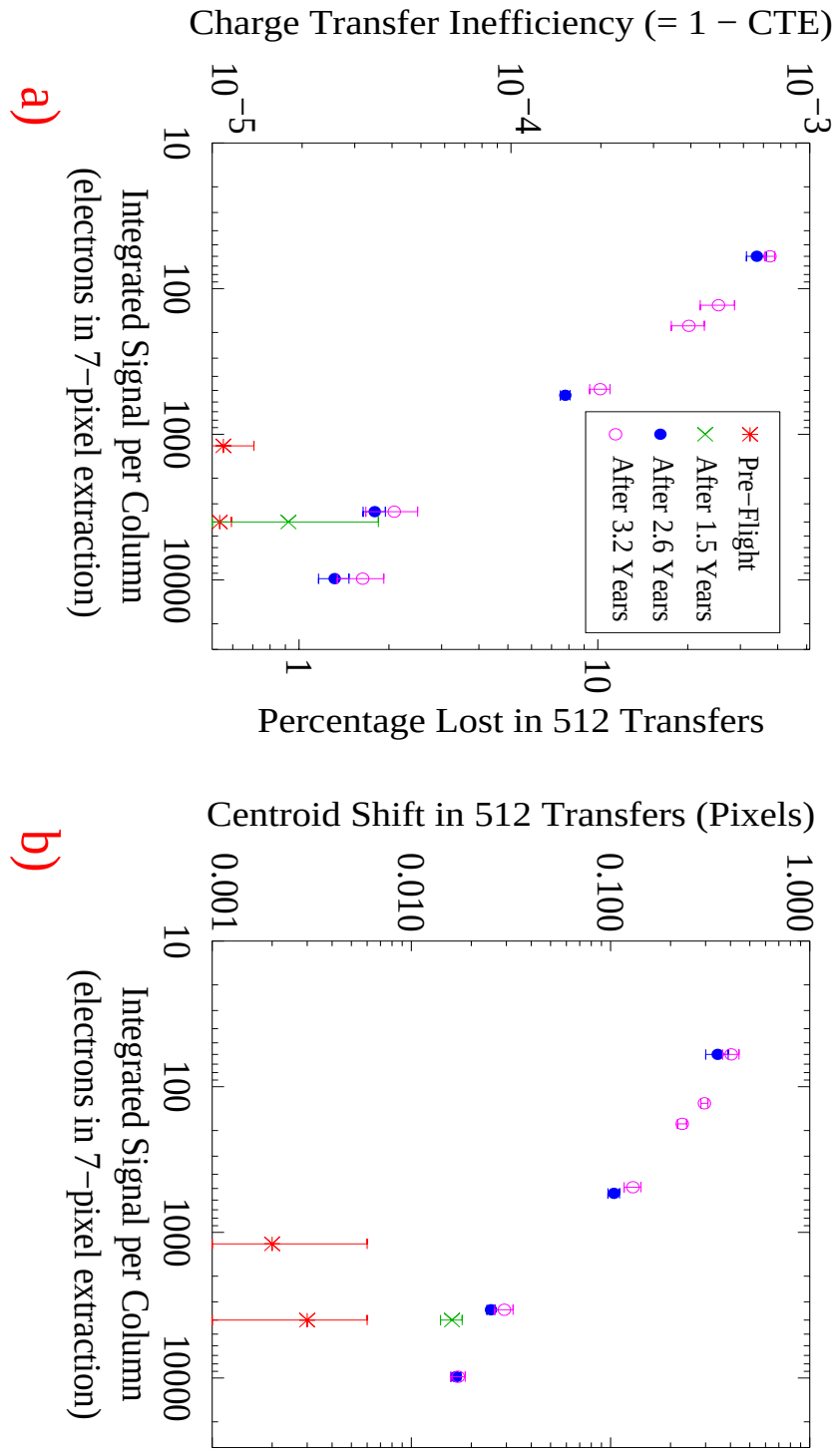

Proposal ID 8415: CCD Sparse-Field CTE External

Execution	Visit 1 executed successfully on Sep. 2, 1999; Visit 2 executed successfully on Sep. 15, 1999; Visit 3 executed successfully on Nov. 6, 1999
Summary of Goals	Measure Charge Transfer Efficiency (CTE) for point sources in a sparse field along the serial and parallel registers, as a function of object intensity and sky background. Use two methods: (a) a bi-directional clocking method, and (b) a phenomenological model first introduced by ***Stetson (1998)***.
Summary of Analysis	The analysis of the data from this program has been discussed and presented by P. Goudfrooij at the "Workshop on Hubble Space Telescope: CCD Detector CTE" (Jan. 31 - Feb. 1, 2000). The proceedings are available at h*ttp://www.stsci.edu/instruments/acs/ctewg/cte_workshop.html*. Updated quantitative results on CTE loss were published in the *IHB, Ch. 7*. An ISR is forthcoming. The CTE loss at chip center is found to increase significantly with time. The CTE loss decreases strongly with increasing source intensity and with increasing sky background. E.g., at a source intensity of 300 electrons, a sky background as modest as ~15 electrons per pixel decreases the CTE loss by more than a factor of two with respect to a sky background of 3 electrons per pixel.
Accuracy Archived	CTE loss accurate to within 1% for signal levels > 200 electrons at the center of the CCD.
Continuation Plans	Continued in Cycle 9 proposals 8839 (for extended sources) and 8854 (for point sources).

Figure 5: Left panel: Charge Transfer Inefficiency (CTI) measurements from external CTE sparse field tests done in Cycles 7 and 8, for different background levels and analysis methods, as a function of source intensity. The 8415 measurements are represented by filled circles and the corresponding curves (see legend). **Right panel:** Parallel-register CTI is derived from the slope of the Amp D/Amp B intensity ratio versus the distance from the B amplifier (i.e., the AXIS2 coordinate). An example is shown here for a source intensity of 400 +/- 100 electrons.

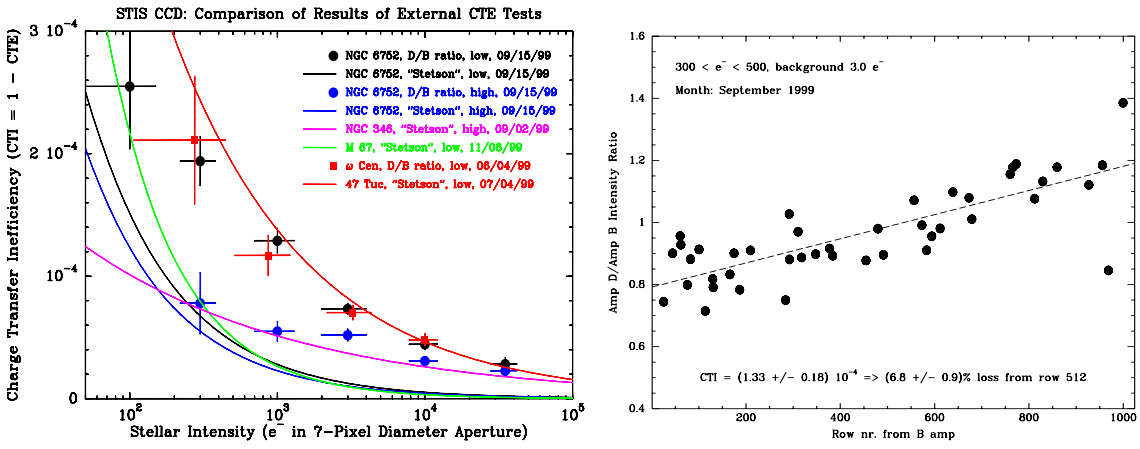

Proposal ID 8416: CCD Full-Field Sensitivity Monitor

Execution	Visits successfully completed in July 1999 and March 2000.
Summary of Goals	A photometric standard star field in Omega Cen is measured in 50CCD mode every six months to monitor CCD sensitivity over the whole field of view. To keep the same stars in the same part of the CCD for every measurement, the spacecraft orientation is kept within a suitable range (+/- 5 deg). The second observation is taken at an orientation rotated by 180 degrees with respect to the other observations.
Summary of Analysis	The data are combined with similar data obtained in previous cycles. A set of stars of different magnitudes at different positions on the detector are selected and aperture photometry carried out for the stars at different epochs.
Accuracy Archived	(a) The magnitudes of the same stars, measured at different positions on the detector show no positional dependence. Also, the analysis was performed for the stars with different luminosities and no luminosity-dependence was found (see the figure). (b) Changes in the magnitude of stars as a function of time over the past three years was found to be less than 1%. (c) The repeatability of the magnitudes of single stars over the past three years (as measured by the rms scatter) is found to be ~1% for brighter stars (m < 20 mag), increasing to 3% for fainter objects. This is likely to be due to background estimates. An ISR is currently being prepared to discuss these in detail.
Continuation Plans	Cycle 9 continuation 8847

Figure 6: Differences between the observed and mean magnitudes (mean of all the available measurements) of stars are plotted as a function of their position on the detector. The relations for stars with different luminosities are shown.

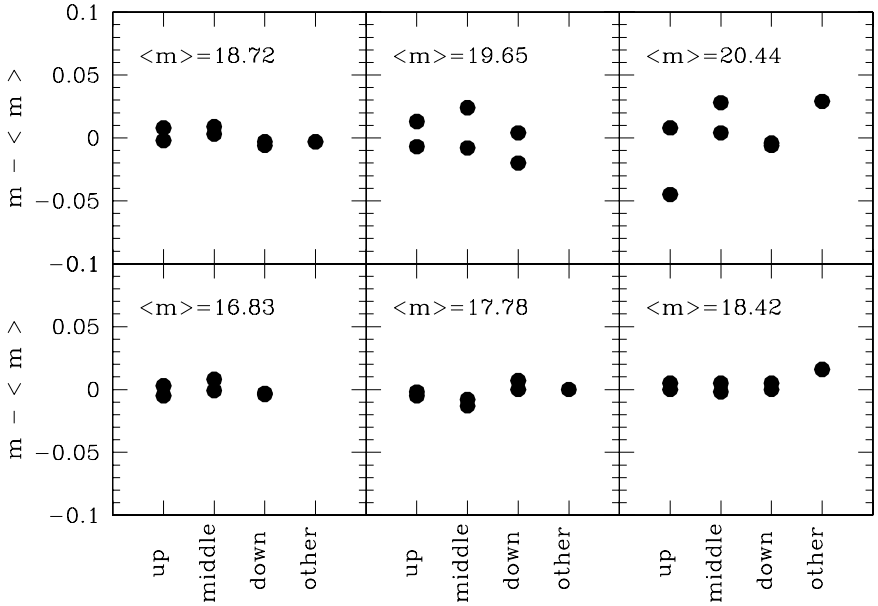

Proposal ID 8417: Slit Wheel Repeatability

Execution	Executed as planned on January 12 2000.
Summary of Goals	Check the stability of the STIS slit wheel from a sequence of comparison lamp spectra using the grating G230MB (centered at 2697 A) and the three smallest long slits (52X0.2, 52X0.1, and 52X0.05)
Summary of Analysis	A total of 23 measurements (given in Table 6 and Figure 7), over a 36 minute period, were obtained with the LINE lamp to check the repeatability of the slit wheel. The data were processed with calstis (the WAVECAL task) through the WAVECORR step, which compares the observed spectra with the template WAVECAL. To remove any error due to MSM non-repeatability, the initial spectra in each aperture were defined as the zeropoint, and the subsequent spectra were corrected to this zeropoint. The results of the dispersion (axis1) direction show a dispersion of 0.06 pixels (3.0 milli-arcsec), while the spatial (axis2) direction shows a dispersion of 0.03 pixels (1.5 milli-arcsec). The values quoted in the Cycle 9 Handbook are 7.4 and 2.5 milli-arcsec for the dispersion and spatial directions, respectively. The values derived in the Cycle 7 check were 2.5 and 1.5 milli-arsec, respectively. There is thus no indication of degradation of the aperture wheel.
Accuracy Archived	Measurements have an accuracy of 0.01 pixels or 0.5 milli-arcseconds.
Continuation Plans	Continued in Cycle 9 proposal 8855

Table 6. Absolute and Relative shifts of Axis1 and Axis2.

Dataset	Aperture	Absolute Shift		Relative Shift		Plot
name		AXIS1	AXIS2	AXIS1	AXIS2	symbol
O5HT01HWQ	52X0.2	-0.240	-2.137	0.000	0.000	1
O5HT01I1Q	52X0.2	-0.386	-2.088	-0.146	0.049	1
O5HT01I2Q	52X0.2	-0.396	-2.108	-0.156	0.029	1
O5HT01I9Q	52X0.2	-0.423	-2.104	-0.183	0.033	1
O5HT01IGQ	52X0.2	-0.404	-2.062	-0.164	0.075	1
O5HT01IMQ	52X0.2	-0.356	-2.051	-0.116	0.086	1
O5HT01IIQ	52X0.2	-0.392	-2.072	-0.152	0.065	1
O5HT01HXQ	52X0.1	-0.218	-2.091	0.000	0.000	2
O5HT01HZQ	52X0.1	-0.267	-2.097	-0.049	-0.006	2
O5HT01I4Q	52X0.1	-0.335	-2.087	-0.117	0.004	2

Dataset	Aperture	Absolute Shift		Relative Shift		Plot
name		AXIS1	AXIS2	AXIS1	AXIS2	symbol
O5HT01I7Q	52X0.1	-0.345	-2.076	-0.127	0.015	2
O5HT01I8Q	52X0.1	-0.346	-2.052	-0.128	0.039	2
O5HT01IAQ	52X0.1	-0.349	-2.082	-0.131	0.009	2
O5HT01IDQ	52X0.1	-0.332	-2.077	-0.114	0.014	2
O5HT01IHQ	52X0.1	-0.316	-2.056	-0.098	0.035	2
O5HT01ILQ	52X0.1	-0.278	-2.081	-0.060	0.010	2
O5HT01HYQ	52X0.05	-0.197	-2.849	0.000	0.000	3
O5HT01I0Q	52X0.05	-0.230	-2.791	-0.033	0.058	3
O5HT01I6Q	52X0.05	-0.281	-2.817	-0.084	0.032	3
O5HT01ICQ	52X0.05	-0.275	-2.809	-0.078	0.040	3
O5HT01IFQ	52X0.05	-0.263	-2.809	-0.066	0.040	3
O5HT01IKQ	52X0.05	-0.231	-2.787	-0.034	0.062	3

Figure 7: The distribution of positions for the STIS slit wheel.

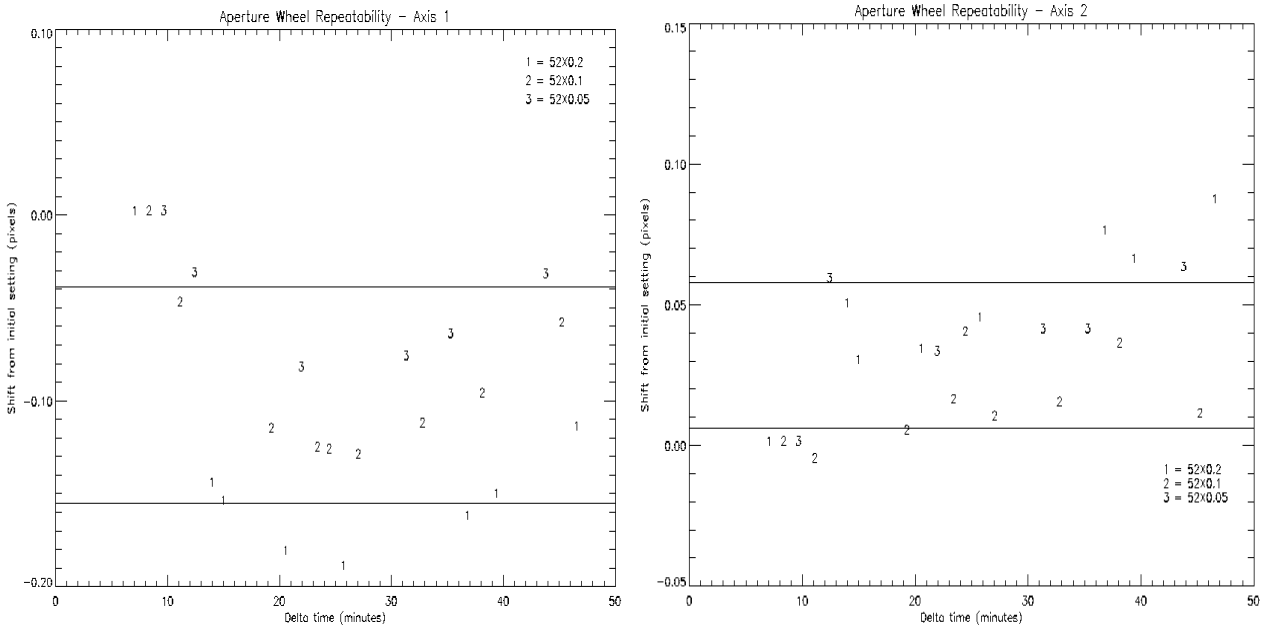

Proposal ID 8418: CCD Sensitivity Monitor

Execution	Executed as planned from Aug 1999 to Aug 2000: 1 orbit every 2 months for the L (low dispersion) modes; orbit every 2 months for the M (medium dispersion) modes.
Summary of Goals	Monitor the Sensitivity of each CCD grating mode to detect any change due to contamination or other causes.
Summary of Analysis	The analysis is reported in the ***STIS ISR 2001-01*** (Stys & Walborn).
Accuracy Archived	The typical sigma of the mean for CCD modes is ~$2x10^{-3}$. The average sigmas of the trend fits (see ISR) is 0.28.
Continuation Plans	Cycle 9 proposal 8856.

Proposal ID 8798: CCD Read Noise Monitor

Execution	This proposal executed once each month in May and June 2000.
Summary of Goals	Follow up on the increased read noise detected in the STIS CCD during SMOV3A by monitoring the read noise in all amplifiers for Gains 1 and 4 and binnings of 1x1, 1x2, 2x1 and 2x2.
Summary of Analysis	Pairs of bias frames were used to measure the read noise by measuring the rms dispersion in a difference image cleaned of discordant pixels via iterative sigma clipping. In some cases, when a pair of images was not available, the noise was measured by fitting a constant to the serial overscan region of the raw image. The read noise in all amplifiers, gains, and binnings was found to be stable at levels consistent with those measured at the end of SMOV3A. In particular, the most heavily used scientific mode (Amp D, Gain=1, bin 1x1) showed the same elevated read noise of 4.4 e-. For comparison, before the safing in the fall of 1999, the read noise in that mode was 4.0 e-.
Accuracy Archived	Typical errors in the read noise measurement are +/-0.05 DN.
Continuation Plans	Regular monitoring continued in Cycle 9 under proposal 8840.

Proposal ID 8799: Calibration of STIS End of Slit Pseudo-Aperture Locations

Execution	This proposal executed once on 4 April 2000.
Summary of Goals	Accurately measure the slit centers at row 900 on the STIS CCD for all 52Xn apertures to enable their use as "pseudo apertures" for observations of compact targets when CTE losses would be a concern. Test the implicit POST-ARG and ACQ/PEAK commands that would be used for accurate target placement at these aperture locations. Confirm spectral traces at these large off center locations.
Summary of Analysis	Obtained spectra and images through the slit at slit center (Y~517) and near the read-out amp (Y~905) of the standard star AGK+81D266 using apertures 52x2, 52x0.5, 52x0.2, 52x0.1, and 52x0.05. Based on a comparison of count rates measured at slit center and near row 900, vignetting is < 2%. Traces at row 905 agree with SMOV2 traces to better than 0.3 pixels. Linear peak-ups at the offset location at row 905 work fine. The angles of the long slits were all determined to be 134.65 degrees. This differed from current entries in the SIAF file, so the entries were updated on 03 July 2000. New entries for the pseudo apertures were inserted with the names 52X2E1, 52X0.5E1, 52X0.2E1, 52X0.1E1, and 52X0.05E1. Since the slits were determined to be slightly curved, the angles associated with the pseudo apertures were set to 134.60 degrees. Full details on the use of the new pseudo apertures is given in the STIS Cycle 10 Phase II Update (http://www.stsci.edu/instruments/stis/proposals/c10_phase2_update.pdf).
Accuracy Archived	Slit centers at row 900 were determined to within 0.1 pixel. Slit angles were determined to within 0.05-0.10 degrees over the full length of the slit.
Continuation Plans	Testing of the implemented pseudo apertures was done in Cycle 9 in proposal 8891.

Proposal ID 8419: CCD Coronographic PSF

Execution	Visit 2 (Mar 2000) only achieved lock using one guide star, and had to be repeated as visit 52 (May 2000). All other visits were successfully executed (June 1999, March 2000, April 2000)
Summary of Goals	To acquire a set of deep, coronographic images of isolated, point source stars with STIS for the purpose of correcting coronographic science observations for residual scattered light from the occulted object, and to test observing strategies for programs that wish to subtract PSF images to search for faint companions or circumstellar material near bright stars.
Summary of Analysis	Primary analysis was done by the STIS-IDT. They concluded that best strategy for searching for faint point source companions is to take images at different roll angles in adjacent orbits; changing rolls in a single orbit produces much poorer results and is an inefficient use of observing time. The STIS-IDT also analyzed the accuracy with which PSFs can be subtracted from each other. A full analysis will be conducted as part of the Cycle 10 calibration outsourcing program 9224 "The Deep Coronographic STIS Point Spread Function" (PI Bruce Woodgate NASA/GSFC).
Accuracy Archived	
Continuation Plans	Additional coronographic images were obtained as part of Cycle 9 programs 8842 and 8844.

Proposal ID 8810: Prism Sensitivity and Faint Calibration Standard Extension

Execution	One visit on July 2000
Summary of Goals	This program is the basic sensitivity measurement for the Prism. Sensitivity measurements were done for the Prism at a central wavelength of 1200 and 2125 A using the 25MAMA and the 2x2 apertures. The faint white dwarf HS2027+0651 is used. Cross-calibration via all first-order L gratings was done as well.
Summary of Analysis	This proposal has been executed, and the analysis has been completed. A new wavelength setting of 2125A for the prism has been added. The prism dispersion solutions and sensitivities for both 1200 and 2125A settings have been derived. The reference files (iac, pct, pht, dsp, 1dt, lmp) are currently being updated accordingly.
Accuracy Archived	The sensitivity measurements were done through a secondary standard, by observing the same star with other first order modes of STIS. The accuracy in the sensitivity measurements is within ~2% relative to the first order modes. The wavelength dispersions in the prism modes vary by a large factor across the detector, but the accuracy is typically 0.2 pix in the central rows.
Continuation Plans	

Proposal ID 8421: Spectroscopic Sensitivity

Execution	Low and Medium resolution: Executed between January 2000 and March 2000. There were 15 visits for the different grating/wavelength combinations. High resolution: All planned exposures were successfully obtained on Feb 29 and Mar 14-19, 2000.
Summary of Goals	Determine spectroscopic sensitivity for all primary central wavelength settings of the medium resolution echelle and some primary wavelength settings of the high resolution echelle. Compare with existing calibration in "_pht" reference files. Look for temporal evolution of sensitivity. If possible interpolating observed sensitivities to model sensitivity of intermediate wavelength settings. Create updated "_pht" reference file.
Summary of Analysis	Low and Medium resolution: The observations executed without problems. Since the data did not provide new information on top of the results from the sensitivity monitor, no analysis was performed. High resolution: Data have been retrieved from the archive and reduced with the new (Aug 2000) echelle scattered light correction algorithm (sc2d). Model spectra of G191B2B have been acquired. A "_pht" reference file pipeline is being developed to automatically process observations into spectroscopic sensitivities. Development work is still required to assess temporal variability and the possibility of interpolating observed sensitivity to intermediate wavelength settings.
Accuracy Archived	Low and Medium resolution: Accuracy of 1% per resolution element (except for extreme wavelengths where the sensitivity falls off). High resolution: Analysis in progress. Anticipate precision much better than 1% and global accuracy of 2%, driven mainly by uncertainties in the model flux spectra that serve as a reference for the calibration.
Continuation Plans	Echelle sensitivity should be monitored approximately every two years to track temporal evolution. A Cycle 10 program is warranted. To track temporal evolution, the following primary wavelength settings should be reobserved: E140M/1425, E230M/2304, E230M/2707, E140H/1234, and E230H/2513. Any additional observations should be at central wavelengths without on-orbit data to better constrain interpolation of echelle sensitivity. Primary wavelength settings should be given precedence. Depending on the final analysis of 8421, it may be possible to use significantly shorter exposure times in future programs

Proposal ID 8422: CCD Imaging Sensitivity & PSF Library

Execution	Visits executed as planned, during Oct 1999, Jun 2000, Jul 2000, and Nov 2000
Summary of Goals	(1) to improve the calibration of the on-axis imaging sensitivity of STIS, (2) to obtain high S/N observations stars (both saturated and unsaturated) for a PSF library, and (3) to obtain narrow-band observations of a star a several detector locations to improve on the STIS PSF model.
Summary of Analysis	1a) Long slit spectra were taken of several hot HB stars in NGC 6681, a cluster used for routine monitoring of the full field sensitivity of broad band MAMA imaging modes (programs 7080, 7132, 7720, 8425, 8858). Flux calibrated spectra have been extracted for these stars and input into SYNPHOT to predict imaging count rates for comparison with data from full field observations. (1b) CCD images of stars of differing spectra types were compared to SYNPHOT predictions. It was found that the previous adjustment to the F28X50LP throughput actually represents an error in the red end sensitivity of the CCD that also affects 50CCD observations. Appropriate adjustments to the filter throughputs and imaging sensitivity are under consideration. (2) A number of images have been coadded to produce deep PSFs and will be input into the PSF library when the library software is ready. (3) Deep F28X50OII images were obtained at various exposure levels and detector positions, and coadded composite images were produced and made available to the Observatory Support Group (OSG) for use in focus modelling. Separate ISRs are in preparation for each of these topics.
Accuracy Archived	For both MAMA and CCD imaging modes we estimate that the data from this program will allow absolute flux calibration to about 5% accuracy. Some improvement to this should be possible, but crowding of the spectra in the NGC 6681 spectra will limit accuracy to at best 2-3%. The most significant correction to currently tabulated values will be for the red end of the CCD imaging sensitivity curve where changes to currently tabulated values will be as large as 30%.
Continuation Plans	Some additional CCD pointed sensitivity observations were taken as part of cycle 9 program 8842. A repeat of the NGC 6681 spectra are planned as part of Cycle 9 program 8849.

Figure 8: Here we compare the difference between predicted and observed magnitudes for a number of stars observed through the 50CCD clear aperture and the F28X50LP filter. Filled circles show the comparison for the currently tabulated CCD imaging sensitivity and the spectroscopically measured F28X50LP relative throughput. Open symbols show the improvement possible by decreasing the CCD sensitivity at wavelengths longer than 5000 A.

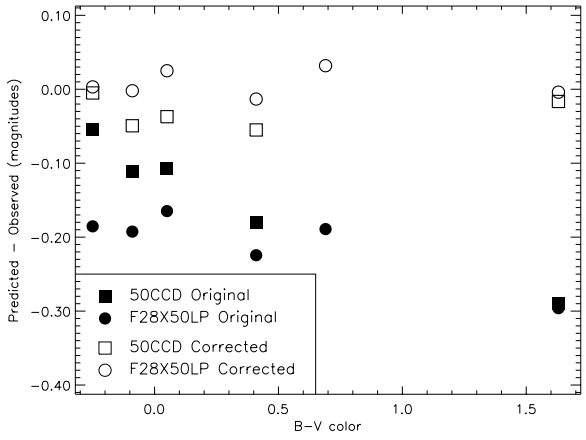

Proposal ID 8423: CCD FASTEX Faint Standards Extension

Execution	Proposal 8423 executed between February 2000 and November 2000. There were 8 visits, with 2 visits per target.
Summary of Goals	Extend the STIS UV sensitivity standards to fainter magnitudes. The new standards will be up to a factor of 10 fainter than current standards and are suitable to support ACS and COS.
Summary of Analysis	The analysis is still ongoing due to the delay in the data acquisition.
Accuracy Archived	The goal is to achieve an accuracy of 1% for the 1st order gratings and 10% for the prism.
Continuation Plans	The program is continued in Cycle 9 under ID 8849.

Proposal ID 8424: MAMA Sensitivity & Focus Monitor

Execution	Executed as planned from Aug 1999 to Aug 2000: 1 orbit every month for the L (low dispersion) modes; 1 orbit every 2 months for the M (medium dispersion) modes; 1 orbit every 6 months for the echelle modes.
Summary of Goals	Monitor the Sensitivity of each MAMA grating mode to detect any change due to contamination or other causes.
Summary of Analysis	The analysis is reported in the ***STIS ISR 2001-01*** (Stys & Walborn).
Accuracy Archived	The typical sigma of the mean for MAMA modes is ~4×10^{-3}. The average sigmas of the trend fits (see ISR) is 0.40.
Continuation Plans	Cycle 9 proposal 8857.

Proposal ID 8425: MAMA Full-Field Sensitivity Monitor

Execution	Visits successfully completed in September 1999 and March 2000
Summary of Goals	Summary of Goals: The purpose of this program is to monitor the sensitivity of the MAMA detectors over the full field by observing the globular cluster NGC6681. The data can be directly compared with similar data obtained in previous cycles.
Summary of Analysis	Aperture photometry was performed on a selected subset of bright stars distributed over the field, as well as for HB stars for which spectra were obtained as part of program 8422. To check the effect of sky background on the estimated magnitudes, different independent techniques were used to measure the sky. An ISR is in preparation for this proposal.
Accuracy Archived	(a) The magnitudes measured for brighter stars (m(ST)~ 16.5) in these images generally show an RMS scatter of 1% (for NUV-SRF2) and 3% (for FUV-25MAMA) between different images taken at the same epoch. The fainter stars (16.5 < m(ST) < 20) with the FUV-25MAMA show a repeatability in magnitudes (at a given epoch) of up to 5%. There is no available measurement for NUV-SRF2 for the stars m(ST) > 16.9. (b) The FUV images show a noticeable time dependence (about -3% per year) that is consistent with the sensitivity losses seen for G140L observations. (c) The magnitudes measured with FUV-F25QTZ show a decrease by ~ -2% per year. There may also be a change in sensitivity as a function of position on the FUV-F25QTZ.
Continuation Plans	Cycle 9 continuation 8858

Figure 9: The repeatability of the magnitudes of the stars, taken as the rms scatter between different exposures taken in a single epoch are plotted as a function of the mean magnitude (mean of all the measurements of a single star in a given epoch). The magnitudes are measured over apertures corresponding to 5 pixels (crosses) and 10 pixels (solid circles). The dashed line is the expected relation, assuming only Poisson noise, for the extreme case of 5 pixels aperture.

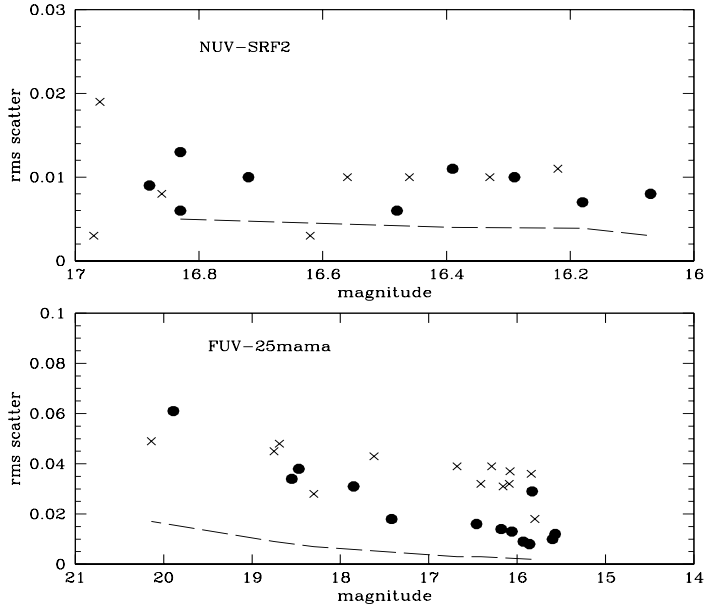

Proposal ID 8426: MAMA Dark Monitor

Execution	Two exposures per week for each MAMA detector.
Summary of Goals	Monitor Dark Current of FUV and NUV MAMA detectors and look for changes in the characteristics of the dark current with time and temperature.
Summary of Analysis	NUV MAMA: Comparison with the simple dark model used in the pipeline shows that this model (dark ~ exp(-12710/T) is still as good a simple approximation as is available. More sophisticated models have been derived that better reproduce the NUV dark behavior under extreme temperature conditions, but they don't significantly improve the dark subtraction for the majority of data. There is also a small systematic change in the shape of the NUV dark with time (at about the 10% level). Time dependant darks have been prepared that may slightly improve the flatness of dark subtracted images, although the improvement is small compared to the normal residuals. FUV MAMA: The FUV MAMA has been previously shown to exhibit an enhanced background glow in the upper left corner at high temperatures. This glow intensity correlates too poorly with time and temperature to allow pipeline subtraction. During cycle 8, the threshold temperature above which the glow appears has shifted significantly downward in temperature. Also two darks, taken at relatively cool temperatures during September 1999 while the NUV MAMA was safed, showed a much higher glow rate than would normally be expected, suggesting that simply cooling the FUV MAMA may not necessarily eliminate the glow. Also, the average number of hot pixels in the FUV darks show a strong increase with time, however, further analysis shows that the number of hot pixels correlates far better with the intensity of the glow than with any other parameter. It is suggested that pipeline FUV darks no longer attempt to subtract hot pixels, but rather simply flag them. New dark files for the pipeline which implement this are in preparation. An ISR describing the new trends in the FUV and NUV MAMA darks is in preparation.
Accuracy Archived	When periods following extended cooling of the NUV MAMA are excluded, the mean observed total NUV dark current varied between roughly 1000 and 1700 counts/sec, and for these same images the pipeline procedure reproduces the observed darks with an RMS scatter of about 10%. In the dark lower right corner of the FUV MAMA, the dark current was essentially independent of time at a rate of 1.2e-4 counts/low-res-pixel/second, while in the glow region the dark rate during cycle 8 averaged about a factor of 6 higher than this.
Continuation Plans	Continued in Cycle 9 by 8843.

Figure 10: The ratio of the measured NUV MAMA dark current to that predicted by the current model implemented in the pipeline is shown as a function of time. While the simple model does not reproduce the strong increase in dark current seen after an extended cooling episode, it does as well as anything in predicting the dark rate for the majority of observations at other times.

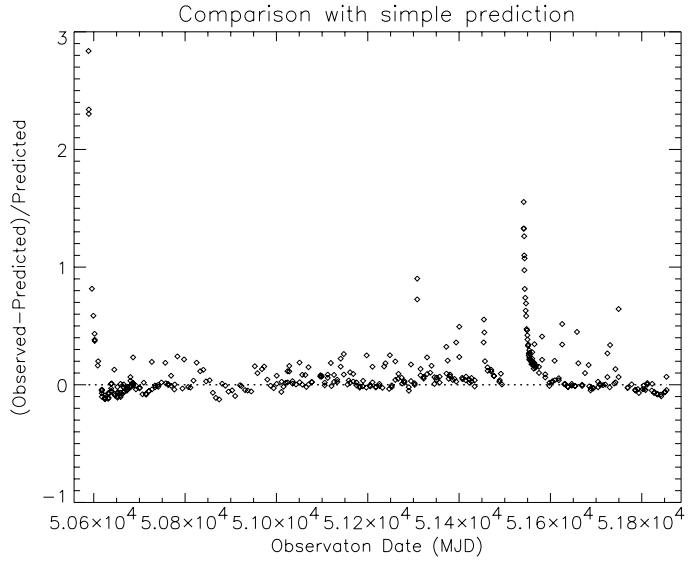

Figure 11: The diamond symbols show the mean dark current (cnts/lo-res-pixel/sec) vs. the OM1CAT temperature as measured in the upper left region of the FUV-MAMA detector where the background glow is the brightest. The + symbols show the rate in the dark lower right corner of the FUV-MAMA. The size of the plotted symbols increase with the date of the observation. Later observations show that the bright glow appears at significantly lower temperatures than it did early in Cycle 7.

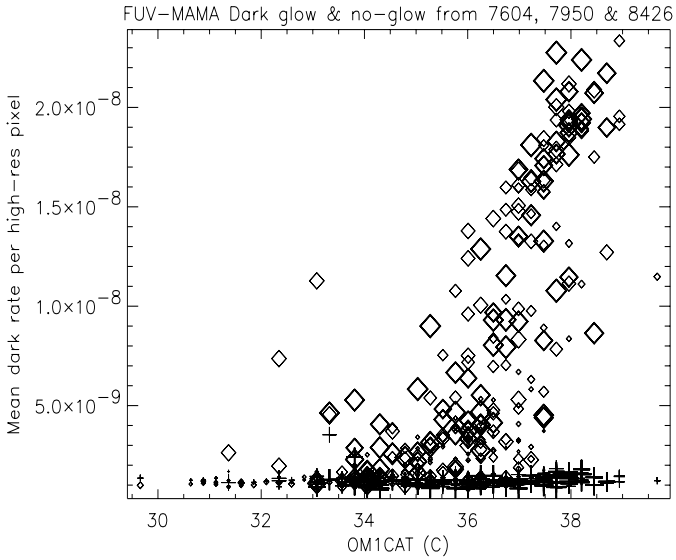

Proposal ID 8427: MAMA Fold Distribution

Execution	Executed during September 1999, April 2000 and October 2000.
Summary of Goals	Measure the distribution of the charge cloud sizes incident upon the anode to monitor the health of the micro-channel plates.
Summary of Analysis	No degradation is apparent (see Fig. 12). The STIS MAMA tubes remain in good health for those parameters measured by the fold analysis. The analysis is described by Long (2001). Procedures and requirements available in the ***TIR 97-09*** and ***ISR 98-02.***
Accuracy Archived	Degradation is measured as a large (more than 20%) deviation between the current and previous measurements.
Continuation Plans	Continued in Cycle 9 proposal 8860

Figure 12: The fold analysis measures the health of the MAMA micro-channel plate. When a photon strikes the MAMA detector it frees a single electron, which accelerates through the micro-channel plate and causes an avalanche of other electrons. The resultant cloud of electrons is collected at the coding electrodes and is interpreted as an event. The contribution of this electron cloud on the electrodes is referred to as the fold. Changes in the fold distribution would indicate a change in the condition of the MAMA tube. The plots for the NUV-MAMA (left) and FUV-MAMA (right) consistently show less than 2% change for the fold number distribution, confirming that the MAMA performance as monitored by the fold analysis has not degraded. The Ball Aerospace (Ball) and GSFC measurements are pre-launch (Long 2001).

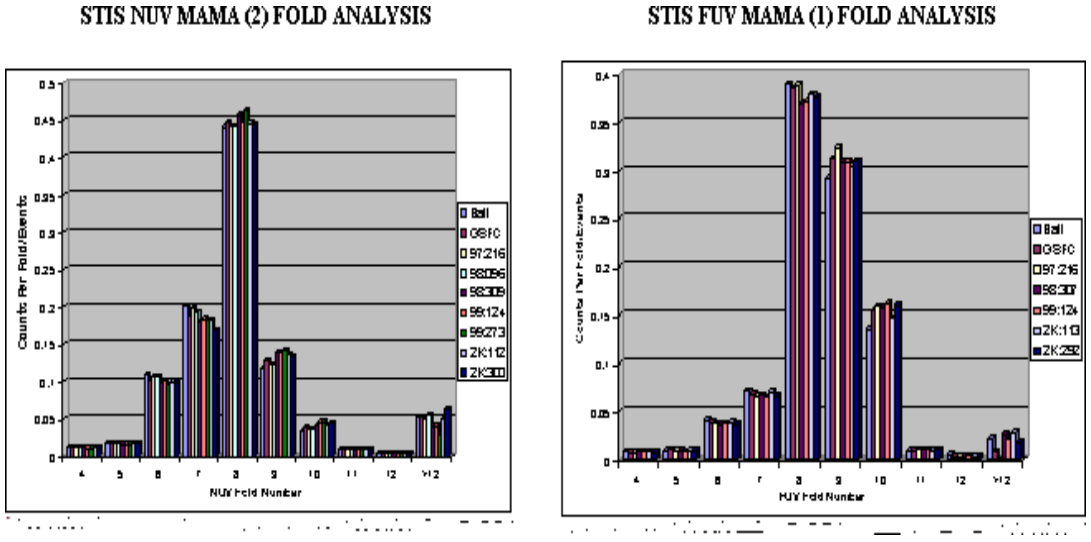

Proposal ID 8428, 8429: MAMA FUV and NUV Flats

Execution	Executed 10 and 11 times, respectively, for FUV and NUV, at approximately weekly intervals. Most visits occurred between 6 Oct 1999 and 2 Mar 2000, though one additional visit for each detector occurred on 8/9 Oct 2000. The original intent was to obtain two epochs of flats, spaced 1 year apart. All visits in the second epoch (except for the first visit) were withdrawn because the decline in the Deuterium and Krypton lamp outputs was great enough that new central wavelength/slit width combinations were warranted to provide greater illumination, and thus preserve lamp lifetime. These changes will be effected in the Cycle 9 follow-on programs.
Summary of Goals	Monitor MAMA pixel-to-pixel flat-field characteristics at the 1% level.
Summary of Analysis	A full analysis is in progress, but there continues to be evolution in the NUV high-res flats in the sense that some of the high-frequency noise is not fully removed. This is consistent with the comparison of ground- and in-flight flats that was performed in Cy 7. There is little or no evolution in the FUV flats, so it is possible that the new p-flat can be combined with the existing, in-flight p-flat to yield a reference file with a S/N approaching 140 per low-res pixel. As well, the FUV spectral flats appear to be very applicable to FUV imaging frames. A TIR on spectral flat construction, and an ISR on MAMA flat-field evolution and applicability are pending.
Accuracy Archived	Approximately 1% per low-resolution element for both detectors.
Continuation Plans	Continued in Cycle 9 as proposals 8862 (FUV) and 8863 (NUV).

Proposal ID 8430: MAMA Dispersion Solutions

Execution	Program executed 3 -- 5 Aug 1999, 3 -- 12 Aug 2000
Summary of Goals	To check and improve on the STIS MAMA dispersion solutions through use of deep engineering wavecals for each FUV and NUV grating (E140H, E140M, E230H, G230M, G140M, G140L, G230M, G230L) using the prime wavelength settings and the 0.2X0.09 or 0.2X0.06 aperture for the echelle modes and the 52X0.1 slit for the first order modes.
Summary of Analysis	Revised dispersion solutions for MAMA and CCD first order modes were received from Don Lindler during Cycle 8. Theses solutions improve on the existing ones in two ways: a) they now incorporate a cubic term in the equation that allows for a better fit to the dispersion curve, and: b) they better represent the dispersion solutions across the whole of the detector, i.e. at points other than near the centerline. Engineering wavecals taken as part of this program, as well as previously, were self-calibrated using the method outlined in ***ISR 1998-12*** and measurements made from spectra extracted at A2 = 512 and A2 = 900 for each image. The following settings were measured using data from both this and previous programs where necessary: G140L 1425; G140M 1173, 1420, 1714; G230L 2376; G230M 1687,2257,3055. The echelle modes were not updated in the new dispersion file delivery, since they show deviations outside the expected range of accuracy, with deviations of several pixels between the observed and expected locations. Since this proposal contains repeat observations made some time apart, direct comparison of the spectra on a setting-by-setting basis was possible. This shows that the echelle wavelengths can show different deviations at different times -- for example, the observations of the E140H 1598 setting o5j202meq and o5j252veq show offsets from the laboratory wavelengths of ~ 0 pixels at 1500 Angstroms, to -2 and +2 pixels, respectively (in the sense of observed - expected), at 1700 Angstroms. Other settings, such as the E230M 1978 setting, give consistent measurements between the two observations, though both sets of measurements show offsets of ~+1 to -0.5 pixels (observed - expected) between the blue and red ends of the detector. These deviations have been traced to a dispersion dependence on the monthly MAMA offset setting, and new dispersion solutions and modifications to the CALSTIS software will be necessary to remedy them. The dispersion solutions for the first-order modes are consistent with, or better than, the stated absolute accuracy in the STIS Instrument Handbook of 0.5 - 1.0 Angstroms. These are all the settings observed in this program: E140H 1425; E140H 1416, 1598, 1271; E230M 1978, 2707; E230H 1813, 2263, 2762; G140L 1425; G140M 1218, 1272, 1420,1567,1714; G230L 2376; 230M 1687, 1933, 2176,2419, 2659, 2898,3055.
Accuracy Archived	First order data is consistent with quoted accuracy of 0.25-0.5 pixels (relative) and 0.5-1.0 pixels (absolute).
Continuation Plans	Cycle 9 proposal 8859

Proposal ID 8431: MAMA Repeller Wire

Execution	Internal visits executed successfully during August and September 1999. Visit 6 failed due to a combination of guide star problems and buffer management problems, and a partial repeat was done in March 2000.
Summary of Goals	Test the limiting resolving power for the FUV MAMA using the Jenkins 0.100x0.030 slit, and confirmation of the Doppler correction for ACCUM mode observations.
Summary of Analysis	Analysis was primarily undertaken by the STIS-IDT as a test of calibration outsourcing (Ted Gull PI). Analysis verified the basic functioning of the procedures for turning off the repeller wire and showed that the improvement in the FUV line spread function is the same as was seen in ground based data. A report describing the results of these tests and the derived line spread functions were delivered by the IDT. Tabular line spread functions are available comparing repeller-on and repeller-off operation. The proposed check of the Doppler correction using the data from the external visits has yet to be done, as does any attempt to compare the external observations with and without the repeller on.
Accuracy Archived	Turning off the repeller wire reduces the wings in the FUV line spread function at cost of reducing the total sensitivity by about 35%. This increases the encircled fraction within +/-2 hi-res pixels along the dispersion direction from 0.72 to 0.82 at 1234 Angstroms and from 0.79 to 0.84 at 1416 Angstroms and longer wavelengths.
Continuation Plans	None.

Proposal ID 8434: MAMA Slitless Spectroscopy

Execution	Program executed 11 - 17 July 2000
Summary of Goals	The purpose of this proposal is to calibrate the dispersion solution as a function of the target-position in slitless spectroscopy for the G140L, G230L and prism modes. Apart from a constant shift, the coefficients of the dispersion solution may depend on the position of target on the detector in slitless model.
Summary of Analysis	None performed yet. A quick-look review of the data shows that most of the G140L 1425 observations resulted in blank datasets as the emission lines in the symbiotic target were moved off the detector when the A1 & A2 shifts were applied. Some of the prism settings are similarly blank. The G230L observations appear to be okay.
Accuracy Archived	
Continuation Plans	

Proposal ID 8433: MAMA Incidence Angle Corrections

Execution

Program executed 12 May -- 17 June 2000

Summary of Goals

To check the accuracy of the correction factors in the _iac reference file that are used to correct the dispersion solution from the arc spectrum aperture to the science spectrum aperture. Generally these correction factors apply a linear shift to the dispersion solution to allow for the offset of the different apertures in the A1 (dispersion) direction. However, some apertures listed in the iac require a first order (stretch) correction to the dispersion solution as well.

To attempt to test the apertures with the most representative settings, the following setting aperture combinations were observed:

Setting	Apertures
E140H 1416	0.2x0.2, 6X0.2, 0.1X0.03, 0.2X0.09
E140M 1425	0.2x0.2, 6X0.2, 0.1X0.03, 0.2X0.06
E230H 2363	0.2X0.2, 0.1X0.09, 6X0.2, 0.1X0.03, 0.1X0.2, 0.2X0.09
E230M 2269	0.2X0.2, 0.1X0.09, 6X0.2, 0.1X0.2, 0.2X0.06
G140L 1425	0.2X0.2, 52X0.05, 52X0.1, 52X0.2, 52X0.5, 52X2, 52X0.2F1
G140M 1165	0.2X0.2, 52X0.05, 52X0.1, 52X0.2, 52X0.5, 52X2, 52X0.2F1
G230L 2376	0.2X0.2, 52X0.05, 52X0.1, 52X0.2, 52X0.5, 52X2, 52X0.2F1
G230M 2338	0.2X0.2, 52X0.05, 52X0.1, 52X0.2, 52X0.5, 52X2, 52X0.2F1

Summary of Analysis

Line lamp observations were made with a range of apertures covering both the reference (0.2x0.2) aperture as well as others with relatively large spatial offsets from the reference. Spectra were extracted from all observations at the spatial location of the 0.2x0.2 aperture. For those spectra where only a linear (zeroth order) correction to the dispersion solution is needed, extracted spectra were converted into IRAF format and cross-correlated using fxcor to determine the pixel offset between each spectrum and the reference for that mode and central wavelength.

Accuracy Archived

Because of the diffuse nature of the line lamp source, measurement accuracy is dependent on the aperture width, with the wider slits providing less accurate results.
Spectral data were calibrated using the same approach as used for testing the dispersion solution accuracy,. Then the 0.2X0.2 (reference) aperture wavelength measurements were subtracted from the measurements for the same lines made with the other apertures. Aside form small linear offsets in the 6X0.2 aperture measurements from those of the reference aperture of less than 0.5 - ~ 1 pixel, partly due to extraction and measurement difficulties with the broad emissionlines, the accuracy of the solutions obtained through the other apertures, namely 0.1X0.2, 0.1X0.03, 0.1X0.09, was excellent, with rms values of < 0.2 pixels.

Continuation Plans

None

Proposal ID 8435: MAMA Echelle LSF Measurements

Execution	Executed in 4 visits during Feb, Mar May and Jul 2000.
Summary of Goals	Measure the LSF for the MAMA Echelle modes.
Summary of Analysis	Calibration spectra were obtained by taking internal line lamp exposures as well as external targets with narrow absorption lines, using narrow slits. The external sources observed for different modes are as follows: E140H and E230M: HD 28497 E230H: HD 89688 E140M: G191B2B Because of a BOP concern, this program had to be carried out in 2-phases: in the first phase, observations were taken with an ND-filter to ensure that there is no BOP violation, followed by the actual observations in the second phase. The observed narrow emission/absorption lines were chosen to produce LSFs, which were convolved with appropriate PSFs to produce LSFs for different slits. The uncertainty in the LSFs are mostly dominated by the uncertainty of our knowledge of the PSFs at different wavelengths, and are typically of the order of 0.2 pix (in FWHM). Example LSFs for the E140M mode are shown. The results were presented at the AAS197 meeting, and are being written as an ISR.
Accuracy Archived	The accuracy is limited by the available PSFs, caused by the limited set of imaging filters for STIS.
Continuation Plans	

Figure 13: LSF for E140M.

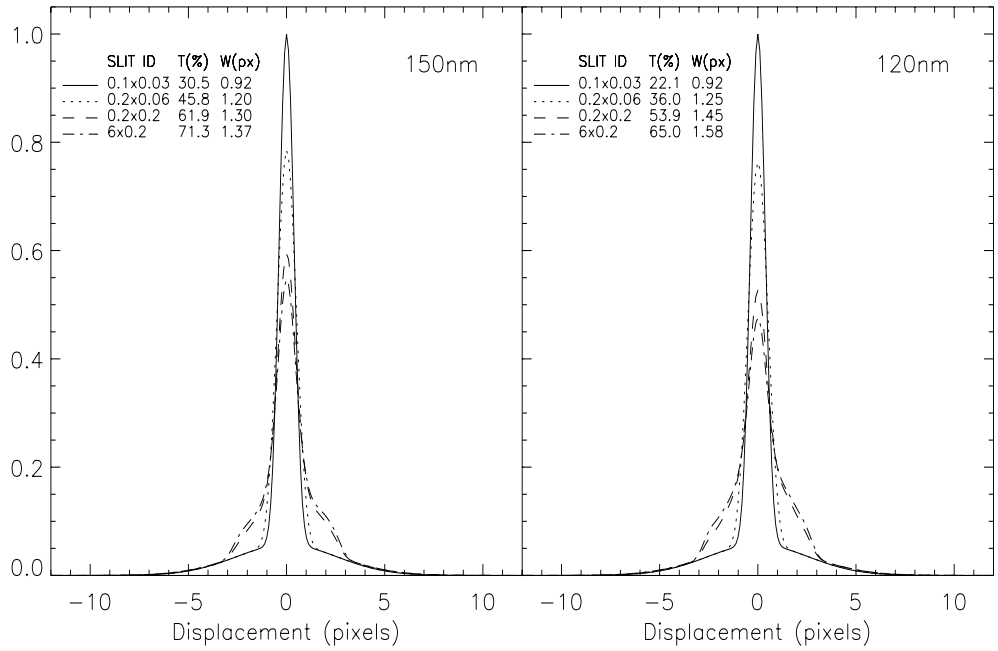

Acknowledgements:

We want to thank Susan Rose for her help in arranging this document.

References

Kimble, R.A., Goudfrooij, P. and Gilliland, R.L. 2000, SPIE, 4013, 532.

Kimble, R.A., et al. 1998, ApJ, 492L, 83

Long, C. 1999a, Draft: STIS Technical Report 99:287 “Orion Nebula Surface Brightness Exceed NUV MAMA Illumination Limits”

Long, C., 2001, Engineering White Paper 01-024

Stetson 1998, PASP, 100, 1448

Woodgate, B.E., et al. 1998, PASP, 110, 1183

Appendix A

STIS Instrument Science Reports (ISRs) are available online at www.stsci.edu/instruments/documents/isrs/:

STIS ISR98-02 “Cycle-7 MAMA Pulse Height Distribution Stability: Fold Analysis Measurement (Revision A)”, H. Ferguson, M. Clampin, V. Argabright

STIS ISR98-12 “Calstis4, calstis11, calstis12: Wavecal Processing in the SITS Calibration Pipeline”, P. Hodge, S.Baum, M. McGrath, S. Hulbert, J. Christensen

STIS ISR98-31 “STIS CCD Performance Monitor Read Noise, Gain, and Consistency of Bias correction during June 1997 - June 1998”, P. Goudfrooij

STIS ISR99-08 “Creation and Testing procedures for STIS CCD Bias reference Files”, P. Goudfrooij

STIS ISR2001-01 “Sensitivity Monitor Report for the STIS First-Order Modes-III”, D. Stys, N.R. Walborn

STIS Technical Instrument Reports (TIRs). A complete list is available from the STIS internal website at ***http://www.stsci.edu/internal/stis/tirs/***. Access may be prohibited for users not employed at STScI (hardcopies can be requested to help@stsci.edu).

STISTIR97-09 “MAMA pulse height distribution stability: Fold Analysis Measurement”, M. Clampin, V. Argabright

STIS TIR98-07 “The STIS Monthly Monitoring Program”, R.Downes, A. Gonnella, R. Katsanis

STIS TIR2000-05 “BIAS Reference Files: Creation Procedures”, R. Diaz-Miller, P. Goudfrooij

STIS TIR2000-06 “CCD DARK Reference File Creation Procedures”, P. Goudfrooij, R. Diaz-Miller